Experimental Eye Research 129 (2014) 93–106

Contents lists available at ScienceDirect

Experimental Eye Research

journal homepage: www.elsevier.com/locate/yexer

Transcriptomic analysis across nasal, temporal, and macular regions of human neural retina and RPE/choroid by RNA-Seq

S. Scott Whitmore [a, b], Alex H. Wagner [a, c], Adam P. DeLuca [a, b], Arlene V. Drack [a, b], Edwin M. Stone [a, b], Budd A. Tucker [a, b], Shemin Zeng [a, b], Terry A. Braun [a, b, c], Robert F. Mullins [a, b], Todd E. Scheetz [a, b, c, *]

[a] Stephen A. Wynn Institute for Vision Research, The University of Iowa, Iowa City, IA, USA
[b] Department of Ophthalmology and Visual Sciences, Carver College of Medicine, The University of Iowa, Iowa City, IA, USA
[c] Department of Biomedical Engineering, College of Engineering, The University of Iowa, Iowa City, IA, USA

ARTICLE INFO

Article history:
Received 14 September 2014
Received in revised form
31 October 2014
Accepted in revised form 4 November 2014
Available online 5 November 2014

Keywords:
RNA-Seq
Retina
Choroid
RPE
Gene expression
Retinitis pigmentosa
Macular degeneration
Transcriptome

ABSTRACT

Proper spatial differentiation of retinal cell types is necessary for normal human vision. Many retinal diseases, such as Best disease and male germ cell associated kinase (*MAK*)-associated retinitis pigmentosa, preferentially affect distinct topographic regions of the retina. While much is known about the distribution of cell types in the retina, the distribution of molecular components across the posterior pole of the eye has not been well-studied. To investigate regional difference in molecular composition of ocular tissues, we assessed differential gene expression across the temporal, macular, and nasal retina and retinal pigment epithelium (RPE)/choroid of human eyes using RNA-Seq. RNA from temporal, macular, and nasal retina and RPE/choroid from four human donor eyes was extracted, poly-A selected, fragmented, and sequenced as 100 bp read pairs. Digital read files were mapped to the human genome and analyzed for differential expression using the Tuxedo software suite. Retina and RPE/choroid samples were clearly distinguishable at the transcriptome level. Numerous transcription factors were differentially expressed between regions of the retina and RPE/choroid. Photoreceptor-specific genes were enriched in the peripheral samples, while ganglion cell and amacrine cell genes were enriched in the macula. Within the RPE/choroid, RPE-specific genes were upregulated at the periphery while endothelium associated genes were upregulated in the macula. Consistent with previous studies, *BEST1* expression was lower in macular than extramacular regions. The *MAK* gene was expressed at lower levels in macula than in extramacular regions, but did not exhibit a significant difference between nasal and temporal retina. The regional molecular distinction is greatest between macula and periphery and decreases between different peripheral regions within a tissue. Datasets such as these can be used to prioritize candidate genes for possible involvement in retinal diseases with regional phenotypes.

1. Introduction

Human visual activities balance the need for high visual acuity, such as reading, driving, and recognizing faces, with comprehensive peripheral vision. High visual acuity is enabled by the macula, a region at the center of the posterior retina with the highest density of cone photoreceptors and ganglion cells. Vision in dim light is made possible by the rod photoreceptor cells which are most concentrated just anterior to the macula.

Many ocular pathologies affect distinct regions of the retina. Macular degenerations, such as age-related macular degeneration, Best disease, Stargardt disease, and North Carolina macular dystrophy, result in loss of photoreceptors and RPE cells in the macula. Other diseases, such as retinitis pigmentosa (RP), cause selective loss of photoreceptors at the periphery of the retina, often sparing central vision until advanced stages of disease. Some diseases manifest further distinction in regional phenotypes. For instance, male germ cell associated kinase (*MAK*)-related RP, the most common cause of inherited blindness among the Ashkenazi Jewish

* Corresponding author. 375 Newton Road, 3181 MERF, The University of Iowa, Iowa City, IA 52242, USA.
E-mail addresses: steven-whitmore@uiowa.edu (S.S. Whitmore), alex-wagner@uiowa.edu (A.H. Wagner), adam-deluca@uiowa.edu (A.P. DeLuca), arlene-drack@uiowa.edu (A.V. Drack), edwin-stone@uiowa.edu (E.M. Stone), budd-tucker@uiowa.edu (B.A. Tucker), shemin-zeng@uiowa.edu (S. Zeng), terry-braun@uiowa.edu (T.A. Braun), robert-mullins@uiowa.edu (R.F. Mullins), todd-scheetz@uiowa.edu (T.E. Scheetz).

http://dx.doi.org/10.1016/j.exer.2014.11.001

Table 1
Donor information. Samples marked by asterisks (*) were analyzed for differential expression in Cuffdiff. Library prep involved poly-A selection.

Donor	Eye	Sex	Age	Cause of death	Death-to-preservation (h)	Retina	RPE/choroid	Library prep.
1*	OS	F	82	Respiratory failure	<4	M, N, T	M, N, T	stranded
2*	OD	M	77	Congestive heart failure	<5	M, N, T	M, N, T	stranded
3*	OD	F	89	Pneumonia	3–4.5	M, N, T	M, N, T	stranded
4*	OS	M	91	Pneumonia	5–6	M, N, T	M, N, T	stranded
5	OD	F	91	Unknown	<6	M, N, T, S, I	–	unstranded

Abbreviations: M– macula; N – nasal; T – temporal; S – superior; I – inferior.

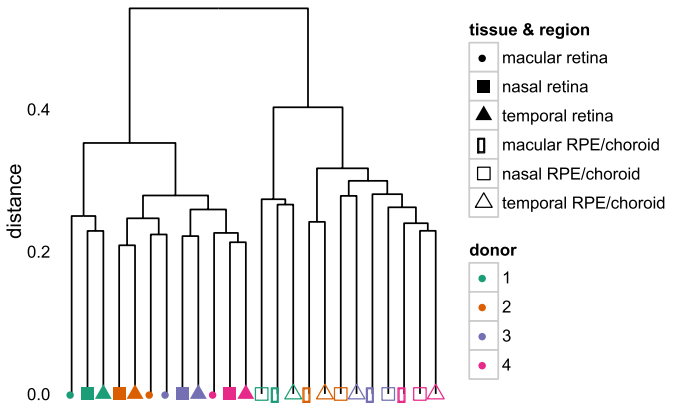

Fig. 1. Hierarchical clustering on expressed isoforms based on Spearman's correlation.

population, manifests an unusual inferonasal predilection for the photoreceptor cell death (Stone et al., 2011; Tucker et al., 2011).

Classic studies on the distribution of cell types through the neural retina (Curcio and Allen, 1990; Curcio et al., 1990; Jonas et al., 1992), combined with extensive disease phenotyping and detailed analyses of single molecule expression have provided substantial insight into the structural and functional organization of the neural retina, retinal pigment epithelium (RPE), and choroid in different regions of the eye. Previous large-scale studies aimed at differentiating macula from periphery have utilized reverse transcriptase-polymerase chain reaction (RT-PCR) (Kociok and Joussen, 2007), array-based technologies (Ishibashi et al., 2004; Diehn et al., 2005; Bowes Rickman et al., 2006; Radeke et al., 2007; van Soest et al., 2007) and more recently, RNA sequencing (RNA-Seq) (Li et al., 2014). Unlike the former two technologies, RNA-Seq provides not only estimates of gene expression level and isoform abundance, but also captures sequence-level information, potentially uncovering novel exons and other transcriptional events.

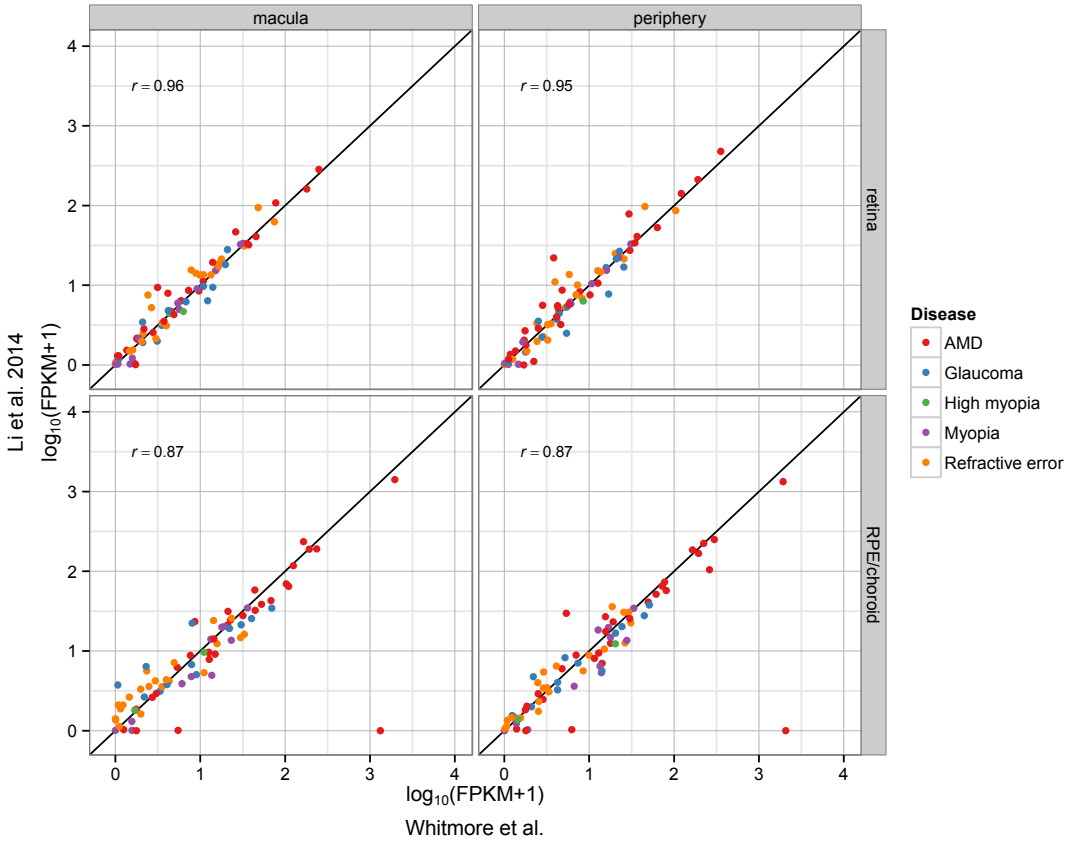

Fig. 2. Comparison of GWAS associated gene sets with data published by Li et al. (2014). The previously published dataset included sclera in the RPE/choroid punches, likely accounting for the number of genes in RPE/choroid below the diagonal. Spearman rank correlation coefficient shown (*r*).

Table 2
Top 40 differentially expressed genes between nasal retina vs. macular retina with q-value < 0.001 and absolute $\log_2$(fold-change) ≥ 1.

Symbol	Description	Chromosome	Start	Stop	Macular retina (FPKM)	Nasal retina (FPKM)	$\log_2$(FC)	P-value	Q-value
HSD17B2	Hydroxysteroid (17-beta) dehydrogenase 2	chr16	82,056,731	82,132,139	1.29	9.55	2.88	5.00E-05	2.86E-04
CYP26B1	Cytochrome P450, family 26, subfamily B, polypeptide 1	chr2	72,356,363	72,375,687	0.41	2.77	2.75	5.00E-05	2.86E-04
COL2A1	Collagen, type II, alpha 1	chr12	48,366,747	48,398,285	1.56	9.98	2.68	5.00E-05	2.86E-04
STEAP4	STEAP family member 4	chr7	87,900,209	87,936,319	0.31	1.89	2.58	5.00E-05	2.86E-04
FOXI3	Forkhead box I3	chr2	88,744,347	88,752,197	0.49	2.81	2.51	5.00E-05	2.86E-04
OXTR	Oxytocin receptor	chr3	8,792,094	8,811,460	0.49	1.91	1.96	5.00E-05	2.86E-04
NPVF	Neuropeptide VF precursor	chr7	25,264,190	25,268,105	29.12	106.31	1.87	5.00E-05	2.86E-04
ZIC1	Zic family member 1	chr3	147,103,834	147,134,784	1.24	4.25	1.78	5.00E-05	2.86E-04
PRL	Prolactin	chr6	22,287,472	22,303,082	4.48	15.15	1.76	5.00E-05	2.86E-04
LOXL4	Lysyl oxidase-like 4	chr10	100,007,442	100,028,007	0.98	3.20	1.71	1.00E-04	5.49E-04
FXYD2[a]	FXYD domain containing ion transport regulator 2	chr11	117,690,789	117,748,201	12.05	35.28	1.55	5.00E-05	2.86E-04
KRT39[b]	Keratin 39	chr17	39,113,368	39,143,387	3.43	10.02	1.55	5.00E-05	2.86E-04
ID3	Inhibitor of DNA binding 3, dominant negative helix-loop-helix protein	chr1	23,884,420	23,886,285	17.01	48.24	1.50	5.00E-05	2.86E-04
EGR1	Early growth response 1	chr5	137,801,180	137,805,004	15.34	39.41	1.36	5.00E-05	2.86E-04
HTR1F	5-hydroxytryptamine (serotonin) receptor 1F, G protein-coupled	chr3	87,841,874	88,049,226	0.78	2.00	1.35	5.00E-05	2.86E-04
CSRP2	Cysteine and glycine-rich protein 2	chr12	77,252,493	77,272,799	19.34	48.16	1.32	5.00E-05	2.86E-04
CYR61	Cysteine-rich, angiogenic inducer, 61	chr1	86,046,443	86,049,648	11.76	29.12	1.31	5.00E-05	2.86E-04
LGALS3	Lectin, galactoside-binding, soluble, 3	chr14	55,595,934	55,612,148	16.89	41.31	1.29	5.00E-05	2.86E-04
C4A[c]	Complement component 4A (Rodgers blood group)	chr6	31,982,571	32,003,195	1.25	3.02	1.27	1.00E-04	5.49E-04
NR4A1	Nuclear receptor subfamily 4, group A, member 1	chr12	52,416,615	52,453,292	15.05	36.28	1.27	1.50E-04	8.01E-04
KCNC2	Potassium voltage-gated channel, Shaw-related subfamily, member 2	chr12	75,433,857	75,603,528	57.75	17.88	−1.69	5.00E-05	2.86E-04
	Potentially novel	chr6	113,745,551	113,755,041	13.32	4.05	−1.72	5.00E-05	2.86E-04
TRPM2	Transient receptor potential cation channel, subfamily M, member 2	chr21	45,770,087	45,869,277	8.60	2.60	−1.72	5.00E-05	2.86E-04
RIT2	Ras-like without CAAX 2	chr18	40,323,182	40,695,841	13.61	4.11	−1.73	5.00E-05	2.86E-04
ISLR2	Immunoglobulin superfamily containing leucine-rich repeat 2	chr15	74,418,236	74,429,152	15.76	4.72	−1.74	5.00E-05	2.86E-04
AHNAK2	AHNAK nucleoprotein 2	chr14	105,371,613	105,444,694	84.49	25.19	−1.75	1.00E-04	5.49E-04
IRX2	Iroquois homeobox 2	chr5	2,745,916	2,751,769	14.95	4.34	−1.78	5.00E-05	2.86E-04
CPNE9	Copine family member IX	chr3	9,745,509	9,771,592	5.89	1.70	−1.79	5.00E-05	2.86E-04
TTC39A	Tetratricopeptide repeat domain 39A	chr1	51,752,172	51,810,785	22.16	6.24	−1.83	5.00E-05	2.86E-04
HTR1B	5-hydroxytryptamine (serotonin) receptor 1B, G protein-coupled	chr6	78,168,875	78,174,100	3.40	0.95	−1.84	1.50E-04	8.01E-04
PHOSPHO1	Phosphatase, orphan 1	chr17	47,300,731	47,308,128	6.47	1.81	−1.84	5.00E-05	2.86E-04
FABP3	Fatty acid binding protein 3, muscle and heart (mammary-derived growth inhibitor)	chr1	31,769,837	31,846,528	131.10	35.95	−1.87	5.00E-05	2.86E-04
PTH1R	Parathyroid hormone 1 receptor	chr3	46,761,072	46,945,351	11.74	3.18	−1.88	1.00E-04	5.49E-04
LCP1	Lymphocyte cytosolic protein 1 (L-plastin)	chr13	46,700,056	46,785,977	7.48	1.94	−1.95	5.00E-05	2.86E-04
SLN	Sarcolipin	chr11	107,578,100	107,582,787	42.78	10.92	−1.97	5.00E-05	2.86E-04
MCTP1	Multiple C2 domains, transmembrane 1	chr5	94,036,882	94,620,279	3.33	0.84	−2.00	5.00E-05	2.86E-04
MRGPRE	MAS-related GPR, member E	chr11	3,246,156	3,254,111	12.08	2.58	−2.22	5.00E-05	2.86E-04
RASGRP3	RAS guanyl releasing protein 3 (calcium and DAG-regulated)	chr2	33,630,960	33,792,285	5.84	1.09	−2.42	5.00E-05	2.86E-04
C1orf170	Chromosome 1 open reading frame 170	chr1	901,876	917,673	8.05	1.37	−2.55	5.00E-05	2.86E-04
PRPH	Peripherin	chr12	49,686,760	49,692,481	55.03	8.39	−2.71	5.00E-05	2.86E-04

[a] FXYD2, FXYD6, and FXYD6-FXYD2 (readthrough) were reported as a single transcriptional locus by Cufflinks.
[b] KRT39 and KRT40 were reported as a single transcriptional locus by Cufflinks.
[c] C4A and C4B_2 were reported as a single transcriptional locus by Cufflinks.

Here we present the first RNA-Seq dataset to investigate the temporal, macular, and nasal regions of the retina and RPE/choroid along with an additional sample with superior and inferior regions represented. Distinct expression profiles clearly differentiated retina from RPE/choroid. Differences between periphery and macula were more pronounced in the retina than in the RPE/choroid and in both tissues reflected dominant cell type distributions. In the neural retina, nasal and temporal regions were indistinguishable by our criteria.

2. Materials and methods

2.1. Tissue acquisition

Human eyes were obtained through the Iowa Lions Eye Bank after informed consent by family members and in accordance with the tenets of the Declaration of Helsinki. Donor information is presented in Table 1. In four donors, an 8 mm trephine punch was used to remove the macula and a 6 mm punch was used to remove

Table 3
Top 40 differentially expressed genes between temporal retina vs. macular retina with q-value < 0.001 and absolute $\log_2$(fold-change) ≥ 1.

Symbol	Description	Chromosome	Start	Stop	Macular retina (FPKM)	Temporal retina (FPKM)	$\log_2$(FC)	P-value	Q-value
MIR1247	MicroRNA 1247	chr14	102,023,301	102,026,828	0.30	4.16	3.77	5.00E-05	2.86E-04
CYP26B1	Cytochrome P450, family 26, subfamily B, polypeptide 1	chr2	72,356,363	72,375,687	0.41	4.68	3.51	5.00E-05	2.86E-04
HSD17B2	Hydroxysteroid (17-beta) dehydrogenase 2	chr16	82,056,731	82,132,139	1.29	10.96	3.08	5.00E-05	2.86E-04
PRL	Prolactin	chr6	22,287,472	22,303,082	4.48	29.37	2.71	5.00E-05	2.86E-04
COL2A1	Collagen, type II, alpha 1	chr12	48,366,747	48,398,285	1.56	9.42	2.59	5.00E-05	2.86E-04
ZIC1	Zic family member 1	chr3	147,103,834	147,134,784	1.24	6.24	2.33	5.00E-05	2.86E-04
NDUFA4L2	NADH dehydrogenase (ubiquinone) 1 alpha subcomplex, 4-like 2	chr12	57,623,324	57,634,949	42.98	162.00	1.91	1.00E-04	5.49E-04
FAM46B	Family with sequence similarity 46, member B	chr1	27,331,510	27,339,333	0.96	3.61	1.91	5.00E-05	2.86E-04
LOXL4	Lysyl oxidase-like 4	chr10	100,007,442	100,028,007	0.98	3.65	1.90	1.00E-04	5.49E-04
FXYD2[a]	FXYD domain containing ion transport regulator 2	chr11	117,690,789	117,748,201	12.05	43.78	1.86	5.00E-05	2.86E-04
ATP1A2	ATPase, Na+/K+ transporting, alpha 2 polypeptide	chr1	160,085,519	160,113,374	17.41	57.10	1.71	5.00E-05	2.86E-04
SIX2	SIX homeobox 2	chr2	45,232,323	45,236,563	2.44	7.92	1.70	5.00E-05	2.86E-04
GPR124	G protein-coupled receptor 124	chr8	37,654,400	37,707,431	4.99	15.61	1.65	5.00E-05	2.86E-04
ADSSL1	Adenylosuccinate synthase like 1	chr14	105,190,533	105,213,663	5.25	15.63	1.57	5.00E-05	2.86E-04
HTR1F	5-hydroxytryptamine (serotonin) receptor 1F, G protein-coupled	chr3	87,841,874	88,049,226	0.78	2.31	1.56	5.00E-05	2.86E-04
ATOH8	Atonal homolog 8 (Drosophila)	chr2	85,978,936	86,018,506	1.13	3.20	1.50	5.00E-05	2.86E-04
NPVF	Neuropeptide VF precursor	chr7	25,264,190	25,268,105	29.12	81.63	1.49	5.00E-05	2.86E-04
PPP1R3C	Protein phosphatase 1, regulatory subunit 3C	chr10	93,379,047	93,392,858	14.02	38.45	1.46	5.00E-05	2.86E-04
CLEC4F	C-type lectin domain family 4, member F	chr2	71,035,775	71,047,732	2.07	5.67	1.45	1.00E-04	5.49E-04
CD4	CD4 molecule	chr12	6,898,637	6,929,977	5.55	14.99	1.43	5.00E-05	2.86E-04
POU4F2	POU class 4 homeobox 2	chr4	147,560,044	147,563,623	11.13	1.98	−2.49	5.00E-05	2.86E-04
NEFM	Neurofilament, medium polypeptide	chr8	24,771,273	24,776,612	544.29	94.76	−2.52	5.00E-05	2.86E-04
SLC17A6	Solute carrier family 17 (vesicular glutamate transporter), member 6	chr11	22,355,132	22,401,046	43.08	7.44	−2.53	5.00E-05	2.86E-04
TTC39A	Tetratricopeptide repeat domain 39A	chr1	51,752,172	51,810,785	22.16	3.76	−2.56	5.00E-05	2.86E-04
ISLR2	Immunoglobulin superfamily containing leucine-rich repeat 2	chr15	74,418,236	74,429,152	15.76	2.61	−2.59	5.00E-05	2.86E-04
POU4F1	POU class 4 homeobox 1	chr13	78,628,989	79,233,323	23.65	3.84	−2.62	5.00E-05	2.86E-04
AHNAK2	AHNAK nucleoprotein 2	chr14	105,371,613	105,444,694	84.49	13.65	−2.63	5.00E-05	2.86E-04
IRX1	Iroquois homeobox 1	chr5	3,596,054	3,601,517	5.55	0.88	−2.66	5.00E-05	2.86E-04
IRX2	Iroquois homeobox 2	chr5	2,745,916	2,751,769	14.95	2.34	−2.67	5.00E-05	2.86E-04
HTR1B	5-hydroxytryptamine (serotonin) receptor 1B, G protein-coupled	chr6	78,168,875	78,174,100	3.40	0.51	−2.74	5.00E-05	2.86E-04
MCTP1	Multiple C2 domains, transmembrane 1	chr5	94,036,882	94,620,279	3.33	0.50	−2.75	5.00E-05	2.86E-04
	Potentially novel	chr6	113,745,551	113,755,041	13.32	1.90	−2.81	5.00E-05	2.86E-04
CPNE9	Copine family member IX	chr3	9,745,509	9,771,592	5.89	0.83	−2.83	5.00E-05	2.86E-04
MRGPRE	MAS-related GPR, member E	chr11	3,246,156	3,254,111	12.08	1.55	−2.96	5.00E-05	2.86E-04
ABO	ABO blood group (transferase A, alpha 1-3-N-acetylgalactosaminyltransferase; transferase B, alpha 1-3-galactosyltransferase)	chr9	136,099,931	136,151,454	3.68	0.44	−3.07	5.00E-05	2.86E-04
	Potentially novel	chr12	108,203,132	108,258,620	3.78	0.45	−3.08	5.00E-05	2.86E-04
RASGRP3	RAS guanyl releasing protein 3 (calcium and DAG-regulated)	chr2	33,630,960	33,792,285	5.84	0.62	−3.24	5.00E-05	2.86E-04
C3orf55	Chromosome 3 open reading frame 55	chr3	157,260,745	157,395,552	6.11	0.60	−3.34	5.00E-05	2.86E-04
PRPH	Peripherin	chr12	49,686,760	49,692,481	55.03	5.00	−3.46	5.00E-05	2.86E-04
C1orf170	Chromosome 1 open reading frame 170	chr1	901,876	917,673	8.05	0.66	−3.60	5.00E-05	2.86E-04

[a] FXYD2, FXYD6, and FXYD6-FXYD2 (readthrough) were reported as a single transcriptional locus by Cufflinks.

temporal and nasal punches. In one additional sample, a 4 mm punch was used to dissect macular, nasal, temporal, superior and inferior punches (Braun et al., 2013). Neural retina and RPE/choroid were separated, flash frozen in liquid nitrogen, and stored at −80 °C. All samples used in this study were preserved in liquid nitrogen within 6 h of death.

2.2. RNA sequencing

RNA was extracted from frozen tissue punches using a Qiagen RNeasy Mini Prep Kit (Qiagen, Valencio, CA) and kept frozen prior to sequencing. The four temporal-macula-nasal sets were prepared for paired-end sequencing using an Illumina TruSeq Stranded mRNA Sample Prep Kit and sequenced on the Illumina platform in the Genomics Division of the Iowa Institute of Human Genetics. Additional paired-end sequencing of one temporal-macula-nasal-superior-inferior sample was performed on the Illumina platform at HudsonAlpha Institute for Biotechnology (Huntsville, AL).

2.3. Bioinformatic analysis

Sequenced reads were mapped to human genome build hg19 using TopHat2 (ver. 2.0.11; (Kim et al., 2013)), transcript structure and abundance were estimated using Cufflinks (ver. 2.1.1; (Trapnell et al., 2010)), and differential expression analysis was performed using Cuffdiff (ver. 2.1.1; (Trapnell et al., 2013)). Quality control analysis was performed using RNA-SeQC (ver. 1.1.7; (DeLuca et al., 2012)). The cummeRbund package (ver. 2.4.1; (Trapnell et al., 2012)) for R (ver. 3.0.2) was used for data visualization. Differential expression analysis was performed for the four donor samples

Table 4
Top 40 differentially expressed genes between nasal RPE/choroid vs. macular RPE/choroid with q-value < 0.001 and absolute $\log_2$(fold-change) ≥ 1.

Symbol	Description	Chromosome	Start	Stop	Macular RPE/choroid (FPKM)	Nasal RPE/choroid (FPKM)	Log2(FC)	*P*-value	*Q*-value
SCG5	Secretogranin V (7B2 protein)	chr15	32,933,869	32,989,298	8.80	117.88	3.74	5.00E-05	2.86E-04
TFPI2	Tissue factor pathway inhibitor 2	chr7	93,514,708	93,545,731	1.87	23.83	3.67	5.00E-05	2.86E-04
FHIT	Fragile histidine triad	chr3	59,733,016	61,237,133	14.79	115.57	2.97	5.00E-05	2.86E-04
RHO	Rhodopsin	chr3	129,247,481	129,254,187	9.49	73.90	2.96	5.00E-05	2.86E-04
MT1G	Metallothionein 1G	chr16	56,700,645	56,701,980	61.09	468.12	2.94	5.00E-05	2.86E-04
GNAT1	Guanine nucleotide binding protein (G protein), alpha transducing activity polypeptide 1	chr3	50,229,042	50,235,129	2.34	16.38	2.81	5.00E-05	2.86E-04
AIPL1	Aryl hydrocarbon receptor interacting protein-like 1	chr17	6,327,058	6,338,519	2.44	16.67	2.77	5.00E-05	2.86E-04
TF	Transferrin	chr3	133,426,380	133,497,850	6.84	46.00	2.75	5.00E-05	2.86E-04
	Potentially	chr2	106,544,607	106,554,533	4.52	28.58	2.66	5.00E-05	2.86E-04
PRSS33	Protease, serine, 33	chr16	2,833,938	2,837,578	1.83	11.43	2.64	5.00E-05	2.86E-04
COL9A2	Collagen, type IX, alpha 2	chr1	40,766,086	40,782,939	3.20	19.90	2.64	5.00E-05	2.86E-04
ATP10B[a]	ATPase, class V, type 10B	chr5	159,990,126	160,365,633	31.64	191.17	2.60	5.00E-05	2.86E-04
RCVRN	Recoverin	chr17	9,801,026	9,808,684	5.57	31.88	2.52	5.00E-05	2.86E-04
SAG	S-antigen; retina and pineal gland (arrestin)	chr2	234,210,734	234,255,703	9.56	53.93	2.50	5.00E-05	2.86E-04
KCNV2	Potassium channel, subfamily V, member 2	chr9	2,717,525	2,730,037	1.88	10.23	2.44	5.00E-05	2.86E-04
SLC4A10	Solute carrier family 4, sodium bicarbonate transporter, member 10	chr2	162,480,844	162,841,786	1.33	6.97	2.39	5.00E-05	2.86E-04
ALDH1A3	Aldehyde dehydrogenase 1 family, member A3	chr15	101,420,008	101,456,897	18.69	96.70	2.37	5.00E-05	2.86E-04
ECEL1	Endothelin converting enzyme-like 1	chr2	233,344,536	233,362,207	1.43	6.55	2.20	5.00E-05	2.86E-04
SFRP1	Secreted frizzled-related protein 1	chr8	41,119,475	41,166,990	13.15	60.45	2.20	5.00E-05	2.86E-04
AKR7A3[b]	Aldo-keto reductase family 7, member A3 (aflatoxin aldehyde reductase)	chr1	19,592,475	19,616,124	0.98	4.06	2.06	1.50E-04	8.01E-04
NRN1	Neuritin 1	chr6	5,998,227	6,008,078	11.86	4.36	−1.44	5.00E-05	2.86E-04
PRIMA1	Proline rich membrane anchor 1	chr14	94,184,643	94,255,079	11.83	4.13	−1.52	5.00E-05	2.86E-04
CXCL14	Chemokine (C-X-C motif) ligand 14	chr5	134,906,370	134,914,969	21.66	7.49	−1.53	5.00E-05	2.86E-04
SCN7A	Sodium channel, voltage-gated, type VII, alpha subunit	chr2	167,260,082	167,350,946	9.90	3.33	−1.57	5.00E-05	2.86E-04
C1QL1	Complement component 1, q subcomponent-like 1	chr17	43,036,339	43,046,605	11.94	3.90	−1.62	1.50E-04	8.01E-04
TRDN	Triadin	chr6	123,537,304	123,958,601	24.71	7.99	−1.63	5.00E-05	2.86E-04
PKHD1L1	Polycystic kidney and hepatic disease 1 (autosomal recessive)-like 1	chr8	110,374,702	110,549,447	6.81	2.19	−1.64	5.00E-05	2.86E-04
GABRE	Gamma-aminobutyric acid (GABA) A receptor, epsilon	chrX	151,121,595	151,143,206	6.17	1.98	−1.64	5.00E-05	2.86E-04
RGS7BP	Regulator of G-protein signaling 7 binding protein	chr5	63,801,626	63,910,486	6.04	1.92	−1.65	5.00E-05	2.86E-04
EPHA3	EPH receptor A3	chr3	89,156,673	89,531,390	11.95	3.72	−1.69	5.00E-05	2.86E-04
CRHBP	Corticotropin releasing hormone binding protein	chr5	76,248,679	76,276,815	6.58	1.97	−1.74	5.00E-05	2.86E-04
CCL14[c]	Chemokine (C–C motif) ligand 14	chr17	34,310,691	34,329,084	208.78	62.35	−1.74	5.00E-05	2.86E-04
CPAMD8	C3 and PZP-like, alpha-2-macroglobulin domain containing 8	chr19	17,003,760	17,137,625	12.55	3.69	−1.77	5.00E-05	2.86E-04
AQP7P1	Aquaporin 7 pseudogene 1	chr9	67,269,284	67,289,625	14.91	4.37	−1.77	5.00E-05	2.86E-04
LOC100507387		chr5	175,542,798	175,554,408	11.01	2.77	−1.99	5.00E-05	2.86E-04
POSTN	Periostin, osteoblast specific factor	chr13	38,136,718	38,172,981	5.91	1.45	−2.02	5.00E-05	2.86E-04
NRXN1	Neurexin 1	chr2	50,145,624	51,259,674	4.18	1.00	−2.06	5.00E-05	2.86E-04
SULT1E1	Sulfotransferase family 1E, estrogen-preferring, member 1	chr4	70,706,929	70,725,870	8.30	1.82	−2.19	5.00E-05	2.86E-04
WFDC1	WAP four-disulfide core domain 1	chr16	84,303,639	84,363,457	154.28	33.71	−2.19	5.00E-05	2.86E-04
TBX15	T-box 15	chr1	119,425,665	119,543,988	5.11	1.08	−2.24	5.00E-05	2.86E-04

[a] ATP10B and LOC285629 were reported as a single transcriptional locus by Cufflinks.
[b] AKR7A3 and AKR7L were reported as a single transcriptional locus by Cufflinks.
[c] CCL14, CCL15, CCL15-CCL14 (readthrough) were reported as a single transcriptional locus by Cufflinks.

with similar processing (macula, temporal, and nasal retina and RPE/choroid). Spearman's rank correlation coefficient as implemented in R was used for all correlations. Genes were deemed differentially expressed if the absolute value of the log2 (fold change) was >1, the q-value < 0.001, and the FPKM (Fragments Per Kilobase of transcript per Million mapped reads) values of either group compared were all > 1.

3. Results

We performed 100 bp paired-end RNA-Seq on retina and RPE/choroid from the temporal, macular, and nasal regions of four clinically normal human donor eyes (Table 1). Hierarchical clustering of samples showed clear separation of neural retina from RPE/choroid samples and evidence of donor effect, i.e., samples derived from the same donor tend to cluster together more often than not (Fig. 1) (Rouhani et al., 2014).

Table 5
Top 40 differentially expressed genes between temporal RPE/choroid vs. macular RPE/choroid with q-value < 0.001 and absolute $\log_2$(fold-change) ≥ 1.

Symbol	Description	Chromosome	Start	Stop	Macular RPE/choroid (FPKM)	Temporal RPE/choroid (FPKM)	$\log_2$(FC)	P-value	Q-value
TFPI2	Tissue factor pathway inhibitor 2	chr7	93,514,708	93,545,731	1.87	82.08	5.45	5.00E-05	2.86E-04
SCG5	Secretogranin V (7B2 protein)	chr15	32,933,869	32,989,298	8.80	118.78	3.75	5.00E-05	2.86E-04
FHIT	Fragile histidine triad	chr3	59,733,016	61,237,133	14.79	194.50	3.72	5.00E-05	2.86E-04
COL9A2	Collagen, type IX, alpha 2	chr1	40,766,086	40,782,939	3.20	25.78	3.01	5.00E-05	2.86E-04
ALDH1A3	Aldehyde dehydrogenase 1 family, member A3	chr15	101,420,008	101,456,897	18.69	139.08	2.90	5.00E-05	2.86E-04
SFRP1	Secreted frizzled-related protein 1	chr8	41,119,475	41,166,990	13.15	91.25	2.79	5.00E-05	2.86E-04
	Potentially novel	chr2	106,544,607	106,554,533	4.52	28.78	2.67	5.00E-05	2.86E-04
ATP10B[a]	ATPase, class V, type 10B	chr5	159,990,126	160,365,633	31.64	181.87	2.52	5.00E-05	2.86E-04
PRSS33	Protease, serine, 33	chr16	2,833,938	2,837,578	1.83	9.95	2.44	5.00E-05	2.86E-04
ECEL1	Endothelin converting enzyme-like 1	chr2	233,344,536	233,362,207	1.43	7.16	2.33	5.00E-05	2.86E-04
VIP	Vasoactive intestinal peptide	chr6	153,054,002	153,080,902	1.91	9.35	2.29	5.00E-05	2.86E-04
MT1G	Metallothionein 1G	chr16	56,700,645	56,701,980	61.09	287.71	2.24	5.00E-05	2.86E-04
PCOLCE2	Procollagen C-endopeptidase enhancer 2	chr3	142,536,701	142,608,045	2.57	12.07	2.23	5.00E-05	2.86E-04
SFRP4	Secreted frizzled-related protein 4	chr7	37,945,534	37,956,525	30.86	125.85	2.03	5.00E-05	2.86E-04
DCN	Decorin	chr12	91,539,034	91,576,806	102.16	403.72	1.98	5.00E-05	2.86E-04
TMEM151A	Transmembrane protein 151A	chr11	66,059,344	66,068,063	1.65	6.39	1.95	5.00E-05	2.86E-04
RD3	Retinal degeneration 3	chr1	211,649,102	211,667,124	1.39	5.29	1.93	5.00E-05	2.86E-04
FABP4	Fatty acid binding protein 4, adipocyte	chr8	82,390,731	82,395,473	8.71	32.59	1.90	5.00E-05	2.86E-04
FXYD3	FXYD domain containing ion transport regulator 3	chr19	35,606,414	35,615,228	24.91	88.14	1.82	5.00E-05	2.86E-04
PKP1	Plakophilin 1	chr1	201,252,579	201,302,121	3.18	10.93	1.78	5.00E-05	2.86E-04
		chr4	145,664,157	145,666,550	10.80	3.89	−1.47	5.00E-05	2.86E-04
AQP1[b]	Aquaporin 1 (Colton blood group)	chr7	30,791,750	30,965,131	142.63	50.74	−1.49	5.00E-05	2.86E-04
NMNAT2	Nicotinamide nucleotide adenylyltransferase 2	chr1	183,217,073	183,387,634	6.38	2.19	−1.54	5.00E-05	2.86E-04
KCNAB1	Potassium voltage-gated channel, shaker-related subfamily, beta member 1	chr3	155,838,336	156,256,927	11.14	3.80	−1.55	5.00E-05	2.86E-04
IGJ	Immunoglobulin J polypeptide, linker protein for immunoglobulin alpha and mu polypeptides	chr4	71,521,257	71,532,652	70.78	23.84	−1.57	5.00E-05	2.86E-04
ITGA8	Integrin, alpha 8	chr10	15,555,950	15,762,323	45.26	15.18	−1.58	5.00E-05	2.86E-04
POSTN	Periostin, osteoblast specific factor	chr13	38,136,718	38,172,981	5.91	1.94	−1.60	5.00E-05	2.86E-04
LOC100507387	Non-coding RNA	chr5	175,542,798	175,554,408	11.01	3.40	−1.70	5.00E-05	2.86E-04
RGS7BP	Regulator of G-protein signaling 7 binding protein	chr5	63,801,626	63,910,486	6.04	1.82	−1.73	5.00E-05	2.86E-04
TBX15	T-box 15	chr1	119,425,665	119,543,988	5.11	1.53	−1.74	5.00E-05	2.86E-04
CPAMD8	C3 and PZP-like, alpha-2-macroglobulin domain containing 8	chr19	17,003,760	17,137,625	12.55	3.68	−1.77	5.00E-05	2.86E-04
PKD1L2	Polycystic kidney disease 1-like 2	chr16	81,134,483	81,253,975	5.61	1.64	−1.78	5.00E-05	2.86E-04
SULT1E1	Sulfotransferase family 1E, estrogen-preferring, member 1	chr4	70,706,929	70,725,870	8.30	2.35	−1.82	5.00E-05	2.86E-04
TMEM132C	Transmembrane protein 132C	chr12	128,751,947	129,192,460	8.78	2.35	−1.90	5.00E-05	2.86E-04
EPHA3	EPH receptor A3	chr3	89,156,673	89,531,390	11.95	2.77	−2.11	5.00E-05	2.86E-04
CRHBP	Corticotropin releasing hormone binding protein	chr5	76,248,679	76,276,815	6.58	1.45	−2.18	5.00E-05	2.86E-04
CXCL14	Chemokine (C-X-C motif) ligand 14	chr5	134,906,370	134,914,969	21.66	4.45	−2.28	5.00E-05	2.86E-04
CALCB	Calcitonin-related polypeptide beta	chr11	15,095,145	15,100,177	7.76	0.99	−2.97	5.00E-05	2.86E-04
WFDC1	WAP four-disulfide core domain 1	chr16	84,303,639	84,363,457	154.28	14.90	−3.37	5.00E-05	2.86E-04
TRDN	Triadin	chr6	123,537,304	123,958,601	24.71	2.33	−3.41	5.00E-05	2.86E-04

[a] ATP10B and LOC285629 were reported as a single transcriptional locus by Cufflinks.
[b] AQP1, FAM188B, INMT, and INMT-FAM188B (readthrough) were reported as a single transcriptional locus by Cufflinks.

Table 6
All differentially expressed genes between temporal RPE/choroid vs. nasal RPE/choroid with q-value < 0.001 and absolute $\log_2$(fold-change) ≥ 1.

Symbol	Description	Chromosome	Start	Stop	Nasal RPE/choroid (FPKM)	Temporal RPE/choroid (FPKM)	$\log_2$(FC)	P-value	Q-value
MPZ	Myelin protein zero	chr1	161,274,410	161,279,793	5.28	40.31	2.93	5.00E-05	2.86E-04
VIP	Vasoactive intestinal peptide	chr6	153,054,002	153,080,902	2.62	9.35	1.84	5.00E-05	2.86E-04
SCN7A	Sodium channel, voltage-gated, type VII, alpha subunit	chr2	167,260,082	167,350,946	3.33	6.72	1.01	1.50E-04	8.01E-04
WFDC1	WAP four-disulfide core domain 1	chr16	84,303,639	84,363,457	33.71	14.90	−1.18	5.00E-05	2.86E-04
HBA2	Hemoglobin, alpha 2	chr16	222,845	223,709	139.35	56.67	−1.30	5.00E-05	2.86E-04
TRDN	triadin	chr6	123,537,304	123,958,601	7.99	2.33	−1.78	5.00E-05	2.86E-04
TULP1	Tubby like protein 1	chr6	35,465,650	35,480,663	7.68	2.21	−1.80	5.00E-05	2.86E-04
TF	Transferrin	chr3	133,426,380	133,497,850	46.00	12.52	−1.88	1.00E-04	5.49E-04
GUCA1B	Guanylate cyclase activator 1B (retina)	chr6	42,151,021	42,168,689	7.48	1.62	−2.21	5.00E-05	2.86E-04
RCVRN	Recoverin	chr17	9,801,026	9,808,684	31.88	4.18	−2.93	5.00E-05	2.86E-04
SAG	S-antigen; retina and pineal gland (arrestin)	chr2	234,210,734	234,255,703	53.93	6.09	−3.15	5.00E-05	2.86E-04
GNAT1	Guanine nucleotide binding protein (G protein), alpha transducing activity polypeptide 1	chr3	50,229,042	50,235,129	16.38	1.54	−3.41	5.00E-05	2.86E-04
AIPL1	Aryl hydrocarbon receptor interacting protein-like 1	chr17	6,327,058	6,338,519	16.67	1.53	−3.44	5.00E-05	2.86E-04
RHO	Rhodopsin	chr3	129,247,481	129,254,187	73.90	6.61	−3.48	5.00E-05	2.86E-04

Table 7
Top 40 differentially expressed genes between macular RPE/choroid vs. macular retina with q-value < 0.001 and absolute $\log_2$(fold-change) ≥ 1.

Symbol	Description	Chromosome	Start	Stop	Macular retina (FPKM)	Macular RPE/choroid (FPKM)	$\log_2$(FC)	P-value	Q-value
	Potentially novel	chr14	106,512,071	106,518,924	0.00	322.59	Inf	5.00E-05	2.86E-04
PRRX2	Paired related homeobox 2	chr9	132,427,911	132,484,952	0.00	60.99	Inf	5.00E-05	2.86E-04
PITX1	Paired-like homeodomain 1	chr5	134,363,350	134,370,461	0.00	25.51	Inf	5.00E-05	2.86E-04
ABCB5	ATP-binding cassette, sub-family B (MDR/TAP), member 5	chr7	20,655,244	20,796,642	0.00	21.83	Inf	5.00E-05	2.86E-04
CCL23	Chemokine (C–C motif) ligand 23	chr17	34,340,096	34,345,026	0.00	21.39	Inf	5.00E-05	2.86E-04
CPXM1	Carboxypeptidase X (M14 family), member 1	chr20	2,774,714	2,781,292	0.00	19.60	Inf	5.00E-05	2.86E-04
	Potentially novel	chr14	106,573,231	106,791,526	0.00	18.70	Inf	5.00E-05	2.86E-04
LOC340357	Long non-coding RNA	chr8	12,623,570	12,675,830	0.00	14.19	Inf	5.00E-05	2.86E-04
	Potentially novel	chr2	72,375,757	72,376,046	0.00	14.09	Inf	5.00E-05	2.86E-04
GZMK	Granzyme K (granzyme 3; tryptase II)	chr5	54,320,106	54,329,960	0.00	9.88	Inf	5.00E-05	2.86E-04
	Potentially novel	chr11	23,099,882	23,100,568	0.00	8.98	Inf	5.00E-05	2.86E-04
SULT1E1	Sulfotransferase family 1E, estrogen-preferring, member 1	chr4	70,706,929	70,725,870	0.00	8.30	Inf	5.00E-05	2.86E-04
CD3E	CD3e molecule, epsilon (CD3-TCR complex)	chr11	118,175,294	118,186,890	0.00	7.73	Inf	5.00E-05	2.86E-04
	Potentially novel	chr9	69,616,397	69,650,111	0.00	6.93	Inf	5.00E-05	2.86E-04
	Potentially novel	chr12	85,380,571	85,386,590	0.00	6.24	Inf	5.00E-05	2.86E-04
KCNK17	Potassium channel, subfamily K, member 17	chr6	39,266,776	39,282,237	0.00	5.88	Inf	5.00E-05	2.86E-04
	Potentially novel	chr5	39,891,795	40,053,420	0.00	4.94	Inf	5.00E-05	2.86E-04
LINC00226	Long intergenic non-protein coding RNA 226	chr14	106,573,231	106,791,526	0.00	4.93	Inf	5.00E-05	2.86E-04
	Potentially novel	chr5	134,374,392	134,375,704	0.00	4.50	Inf	5.00E-05	2.86E-04
CTSG	Cathepsin G	chr14	25,042,723	25,045,466	0.00	4.32	Inf	5.00E-05	2.86E-04
	Potentially novel	chr16	84,273,764	84,281,615	3.58	0.00	-Inf	5.00E-05	2.86E-04
DEFB131	Defensin, beta 131	chr4	9,446,259	9,452,240	3.61	0.00	-Inf	5.00E-05	2.86E-04
	Potentially novel	chr4	147,559,182	147,559,943	3.65	0.00	-Inf	5.00E-05	2.86E-04
	Potentially novel	chr14	48,702,743	48,793,893	3.69	0.00	-Inf	5.00E-05	2.86E-04
	Potentially novel	chr7	21,181,327	21,253,288	3.82	0.00	-Inf	5.00E-05	2.86E-04
LRTM2	Leucine-rich repeats and transmembrane domains 2	chr12	1,901,122	2,032,895	4.46	0.00	-Inf	1.00E-04	5.49E-04
	Potentially novel	chr3	76,359,774	76,360,809	4.76	0.00	-Inf	5.00E-05	2.86E-04
	Potentially novel	chr12	55,403,375	55,409,332	5.28	0.00	-Inf	5.00E-05	2.86E-04
	Potentially novel	chr20	61,785,077	61,787,572	5.67	0.00	-Inf	5.00E-05	2.86E-04
DSCR8	Down syndrome critical region gene 8	chr21	39,493,544	39,528,605	5.99	0.00	-Inf	5.00E-05	2.86E-04
TRPC7	Transient receptor potential cation channel, subfamily C, member 7	chr5	135,548,424	135,732,845	7.25	0.00	-Inf	5.00E-05	2.86E-04
CCDC172	Coiled-coil domain containing 172	chr10	118,083,939	118,139,551	7.56	0.00	-Inf	5.00E-05	2.86E-04
	Potentially novel	chr8	55,506,068	55,508,509	8.16	0.00	-Inf	5.00E-05	2.86E-04
	Potentially novel	chr1	23,280,951	23,299,340	9.02	0.00	-Inf	5.00E-05	2.86E-04
FEZF2	FEZ family zinc finger 2	chr3	62,355,295	62,360,692	9.07	0.00	-Inf	5.00E-05	2.86E-04
	Potentially novel	chr18	5,847,207	5,876,306	9.92	0.00	-Inf	5.00E-05	2.86E-04
POU4F2	POU class 4 homeobox 2	chr4	147,560,044	147,563,623	11.13	0.00	-Inf	5.00E-05	2.86E-04
	Potentially novel	chr5	178,422,323	178,423,333	12.42	0.00	-Inf	5.00E-05	2.86E-04
CACNG3	Calcium channel, voltage-dependent, gamma subunit 3	chr16	24,266,873	24,373,737	16.08	0.00	-Inf	5.00E-05	2.86E-04
	Potentially novel	chr12	9,727,536	9,728,249	30.87	0.00	-Inf	5.00E-05	2.86E-04

3.1. Comparison with previously published data

We compared our dataset to a recently published table of FPKM (Fragments Per Kilobase of transcript per Million mapped reads) values derived from macular and peripheral retina and RPE/choroid/sclera for 91 genes implicated by genome-wide association studies (GWAS) in various eye diseases (Li et al., 2014). To compare the previous results to ours, we averaged our nasal and temporal FPKM values together for one "peripheral" value (Fig. 2). Where Cufflinks matched two separate loci to a single gene symbol, we took the higher of the two values. While the values for retina roughly follow the diagonal, FPKM values were consistently higher for genes in our RPE/choroid samples compared to the RPE/choroid/sclera samples of Li et al., likely reflecting the cellular paucity of the sclera. The obvious exception is *COL10A1*, which shows higher expression in peripheral RPE/choroid/sclera than in peripheral RPE/choroid alone. In addition, *TIMP3*, reported by Li et al. as a predominantly retinal transcript, showed robust expression in all RPE/choroid samples in the current report (Fig. 2).

3.2. Regional gene expression by tissue

To evaluate gene expression across regions of the retina and RPE/choroid, we used Cuffdiff to perform pairwise tests between groups of punches (Supplemental Table 1). When comparing nasal

Table 8
Top 40 differentially expressed genes between nasal RPE/choroid vs. nasal retina with q-value < 0.001 and absolute $\log_2$(fold-change) ≥ 1.

Symbol	Description	Chromosome	Start	Stop	Nasal retina (FPKM)	Nasal RPE/choroid (FPKM)	$\log_2$(FC)	P-value	Q-value
	Potentially novel	chr14	106,512,071	106,518,924	0.00	142.27	Inf	5.00E-05	2.86E-04
PITX1	Paired-like homeodomain 1	chr5	134,363,350	134,370,461	0.00	19.53	Inf	5.00E-05	2.86E-04
LOC340357	Long non-coding RNA	chr8	12,623,570	12,675,830	0.00	10.88	Inf	5.00E-05	2.86E-04
GZMK	Granzyme K (granzyme 3; tryptase II)	chr5	54,320,106	54,329,960	0.00	8.65	Inf	5.00E-05	2.86E-04
KCNK17	Potassium channel, subfamily K, member 17	chr6	39,266,776	39,282,237	0.00	8.45	Inf	5.00E-05	2.86E-04
CCL23	Chemokine (C−C motif) ligand 23	chr17	34,340,096	34,345,026	0.00	7.03	Inf	5.00E-05	2.86E-04
	Potentially novel	chr5	39,891,795	40,053,420	0.00	6.18	Inf	5.00E-05	2.86E-04
TEX41	Testis expressed 41 (non-protein coding)	chr2	145,425,533	146,021,001	0.00	5.35	Inf	5.00E-05	2.86E-04
	Potentially novel	chr14	22,320,484	22,323,708	0.00	4.66	Inf	5.00E-05	2.86E-04
	Potentially novel	chr5	134,374,392	134,375,704	0.00	3.67	Inf	5.00E-05	2.86E-04
KLRB1	Killer cell lectin-like receptor subfamily B, member 1	chr12	9,747,869	9,760,497	0.00	3.53	Inf	5.00E-05	2.86E-04
CCL13	Chemokine (C−C motif) ligand 13	chr17	32,683,470	32,685,629	0.00	3.52	Inf	5.00E-05	2.86E-04
	Potentially novel	chr18	3,466,243	3,478,970	0.00	2.99	Inf	5.00E-05	2.86E-04
LMX1B	LIM homeobox transcription factor 1, beta	chr9	129,376,673	129,463,311	0.00	2.93	Inf	5.00E-05	2.86E-04
SLAMF7	SLAM family member 7	chr1	160,709,032	160,725,021	0.00	1.57	Inf	5.00E-05	2.86E-04
ZG16B	Zymogen granule protein 16B	chr16	2,880,172	2,882,285	0.00	1.53	Inf	5.00E-05	2.86E-04
SAA1	Serum amyloid A1	chr11	18,287,807	18,291,523	0.45	2255.58	12.30	5.00E-05	2.86E-04
PLA2G2A	Phospholipase A2, group IIA (platelets, synovial fluid)	chr1	20,301,923	20,306,932	0.27	553.86	11.01	5.00E-05	2.86E-04
ABCB5	ATP-binding cassette, sub-family B (MDR/TAP), member 5	chr7	20,655,244	20,796,642	0.01	18.83	10.65	1.50E-04	8.01E-04
PLVAP	Plasmalemma vesicle associated protein	chr19	17,462,251	17,488,137	0.09	122.71	10.47	5.00E-05	2.86E-04
KCNC2	Potassium voltage-gated channel, Shaw-related subfamily, member 2	chr12	75,433,857	75,603,528	17.88	0.18	−6.60	5.00E-05	2.86E-04
NEFM	Neurofilament, medium polypeptide	chr8	24,771,273	24,776,612	169.15	1.71	−6.63	5.00E-05	2.86E-04
CNGA3	Cyclic nucleotide gated channel alpha 3	chr2	98,703,594	99,016,789	4.16	0.04	−6.67	5.00E-05	2.86E-04
RASGRF1	Ras protein-specific guanine nucleotide-releasing factor 1	chr15	79,252,288	79,383,265	14.36	0.14	−6.69	5.00E-05	2.86E-04
CACNG5	Calcium channel, voltage-dependent, gamma subunit 5	chr17	64,831,229	64,890,871	19.03	0.18	−6.72	5.00E-05	2.86E-04
AGBL4	ATP/GTP binding protein-like 4	chr1	48,998,369	50,489,626	2.06	0.02	−6.76	5.00E-05	2.86E-04
	Potentially novel	chr10	3,675,719	3,690,589	7.93	0.05	−7.41	5.00E-05	2.86E-04
CRYAA	Crystallin, alpha A	chr21	44,570,160	44,592,913	318.89	1.65	−7.59	5.00E-05	2.86E-04
C6orf7	Chromosome 6 open reading frame 7	chr6	80,472,023	80,580,137	2.24	0.01	−8.22	5.00E-05	2.86E-04
	Potentially novel	chr6	89,881,239	89,881,908	1.30	0.00	-Inf	5.00E-05	2.86E-04
LEMD1	LEM domain containing 1	chr1	205,342,379	205,436,588	1.54	0.00	-Inf	5.00E-05	2.86E-04
	Potentially novel	chr9	32,865,800	32,909,556	2.00	0.00	-Inf	5.00E-05	2.86E-04
	Potentially novel	chr17	5,000,474	5,000,915	2.59	0.00	-Inf	5.00E-05	2.86E-04
	Potentially novel	chr11	3,599,999	3,602,427	2.82	0.00	-Inf	5.00E-05	2.86E-04
	Potentially novel	chr1	10,873,924	10,874,785	3.12	0.00	-Inf	5.00E-05	2.86E-04
	Potentially novel	chr16	84,273,764	84,281,615	3.15	0.00	-Inf	5.00E-05	2.86E-04
	Potentially novel	chr1	91,183,265	91,183,539	3.39	0.00	-Inf	5.00E-05	2.86E-04
C1orf141	Chromosome 1 open reading frame 141	chr1	67,557,494	67,607,567	3.55	0.00	-Inf	5.00E-05	2.86E-04
	Potentially novel	chr10	81,657,061	81,657,275	3.67	0.00	-Inf	5.00E-05	2.86E-04
DEFB131	Defensin, beta 131	chr4	9,446,259	9,452,240	4.55	0.00	-Inf	5.00E-05	2.86E-04

retina vs. macular retina, 30 genes showed increased expression in nasal retina and 128 genes showed decreased expression (Table 2). When comparing temporal retina vs. macular retina, 37 genes showed increased expression in temporal retina and 323 genes showed decreased expression (Table 3). Notably, of the 40 top differences in expression between nasal retina and macular retina (Table 2), 21 of the same genes were in the list of top 40 differences between temporal retina and macular retina (Table 3). Interestingly, no genes were differentially expressed between temporal and nasal retina, suggesting that these two regions of the retina are molecularly indistinguishable using these criteria.

In the nasal vs. macular RPE/choroid comparison, 81 genes showed increased expression in the nasal RPE/choroid and 39 genes showed decreased expression (Table 4). When comparing temporal vs. macular RPE/choroid, 70 genes were increased in the temporal RPE/choroid and 44 genes were decreased (Table 5). In contrast to the retina, in which no gene expression differences between different peripheral regions met our criteria for

Table 9
Top 40 differentially expressed genes between temporal RPE/choroid vs. temporal retina with q-value < 0.001 and absolute $\log_2$(fold-change) ≥ 1.

Symbol	Description	Chromosome	Start	Stop	Temporal retina (FPKM)	Temporal RPE/choroid (FPKM)	$\log_2$(FC)	P-value	Q-value
	Potentially novel	chr14	106,512,071	106,518,924	0.00	192.09	Inf	5.00E-05	2.86E-04
PITX1	Paired-like homeodomain 1	chr5	134,363,350	134,370,461	0.00	19.83	Inf	5.00E-05	2.86E-04
LOC340357	Long non-coding RNA	chr8	12,623,570	12,675,830	0.00	14.87	Inf	5.00E-05	2.86E-04
PAX3	Paired box 3	chr2	223,064,605	223,169,936	0.00	13.21	Inf	5.00E-05	2.86E-04
AKR1B10	Aldo-keto reductase family 1, member B10 (aldose reductase)	chr7	134,200,788	134,226,166	0.00	8.67	Inf	5.00E-05	2.86E-04
GZMK	Granzyme K (granzyme 3; tryptase II)	chr5	54,320,106	54,329,960	0.00	8.60	Inf	5.00E-05	2.86E-04
	Potentially novel	chr1	170,632,134	170,633,074	0.00	8.30	Inf	5.00E-05	2.86E-04
	Potentially novel	chr5	39,891,795	40,053,420	0.00	7.70	Inf	5.00E-05	2.86E-04
FOXD3	Forkhead box D3	chr1	63,786,575	63,790,797	0.00	6.14	Inf	5.00E-05	2.86E-04
TEX41	Testis expressed 41 (non-protein coding)	chr2	145,425,533	146,021,001	0.00	5.47	Inf	5.00E-05	2.86E-04
	Potentially novel	chr11	23,099,882	23,100,568	0.00	5.43	Inf	5.00E-05	2.86E-04
CLEC10A	C-type lectin domain family 10, member A	chr17	6,977,855	6,983,826	0.00	4.53	Inf	5.00E-05	2.86E-04
LCK	LCK proto-oncogene, Src family tyrosine kinase	chr1	32,716,839	32,751,766	0.00	3.57	Inf	5.00E-05	2.86E-04
LMX1B	LIM homeobox transcription factor 1, beta	chr9	129,376,673	129,463,311	0.00	3.50	Inf	5.00E-05	2.86E-04
	Potentially novel	chr9	69,616,397	69,650,111	0.00	3.46	Inf	5.00E-05	2.86E-04
S1PR5	Sphingosine-1-phosphate receptor 5	chr19	10,623,417	10,628,668	0.00	3.27	Inf	5.00E-05	2.86E-04
CLIC3	Chloride intracellular channel 3	chr9	139,889,059	139,891,024	0.00	3.18	Inf	5.00E-05	2.86E-04
	Potentially novel	chr5	134,374,392	134,375,704	0.00	3.17	Inf	5.00E-05	2.86E-04
	Potentially novel	chr18	3,466,243	3,478,970	0.00	2.72	Inf	5.00E-05	2.86E-04
CCL13	Chemokine (C–C motif) ligand 13	chr17	32,683,470	32,685,629	0.00	2.56	Inf	5.00E-05	2.86E-04
	Potentially novel	chr11	117,673,186	117,673,498	3.81	0.00	-Inf	5.00E-05	2.86E-04
C1orf141	Chromosome 1 open reading frame 141	chr1	67,557,494	67,607,567	3.83	0.00	-Inf	5.00E-05	2.86E-04
	Potentially novel	chr18	76,736,580	76,739,475	4.33	0.00	-Inf	5.00E-05	2.86E-04
NAT16	N-acetyltransferase 16 (GCN5-related, putative)	chr7	100,813,667	100,823,557	4.36	0.00	-Inf	5.00E-05	2.86E-04
C16orf11	Chromosome 16 open reading frame 11	chr16	610,179	615,529	4.39	0.00	-Inf	5.00E-05	2.86E-04
	Potentially novel	chr12	55,403,375	55,409,332	4.56	0.00	-Inf	5.00E-05	2.86E-04
	Potentially novel	chr1	10,873,924	10,874,785	4.76	0.00	-Inf	5.00E-05	2.86E-04
	Potentially novel	chr17	77,818,917	77,825,465	4.77	0.00	-Inf	5.00E-05	2.86E-04
	Potentially novel	chr3	192,862,226	192,894,687	5.02	0.00	-Inf	5.00E-05	2.86E-04
DEFB131	Defensin, beta 131	chr4	9,446,259	9,452,240	5.46	0.00	-Inf	5.00E-05	2.86E-04
	Potentially novel	chr7	127,116,864	127,146,567	6.15	0.00	-Inf	5.00E-05	2.86E-04
	Potentially novel	chr7	21,181,327	21,253,288	6.30	0.00	-Inf	5.00E-05	2.86E-04
	Potentially novel	chr1	23,280,951	23,299,340	6.93	0.00	-Inf	5.00E-05	2.86E-04
MIR124-3	MicroRNA 124-3	chr20	61,808,787	61,813,324	6.97	0.00	-Inf	5.00E-05	2.86E-04
	Potentially novel	chr20	61,785,077	61,787,572	9.70	0.00	-Inf	5.00E-05	2.86E-04
	Potentially novel	chr8	55,506,068	55,508,509	11.21	0.00	-Inf	5.00E-05	2.86E-04
	Potentially novel	chr5	178,422,323	178,423,333	11.40	0.00	-Inf	5.00E-05	2.86E-04
	Potentially novel	chr9	2,734,043	2,734,455	16.22	0.00	-Inf	5.00E-05	2.86E-04
DEFB119	Defensin, beta 119	chr20	29,964,965	29,978,452	56.91	0.00	-Inf	5.00E-05	2.86E-04
	Potentially novel	chr12	9,727,536	9,728,249	58.97	0.00	-Inf	5.00E-05	2.86E-04

differential expression, three genes (*MPZ*, *VIP*, and *SCN7A*) were increased in the nasal RPE/choroid and 11 were decreased when comparing temporal vs. nasal RPE/choroid (Table 6). Higher expression of neuroretinal genes (e.g., *RHO*, *RCVRN*, *SAG*) in the nasal RPE/choroid group as compared to the macular (Table 4) or temporal (Table 6) RPE/choroid groups is traceable to the slight but detectable neuroretinal contamination of the nasal RPE/choroid from donor 2.

We also performed comparisons between tissues within a region. We observed 2747 genes with increased expression and 2053 genes with decreased expression when comparing macular RPE/choroid vs. macular retina (Table 7). We observed 2842 genes with increased expression and 1935 genes with decreased expression when comparing nasal RPE/choroid vs. nasal retina (Table 8). We observed 2762 genes with increased expression and 1909 genes with decreased expression when comparing temporal RPE/choroid

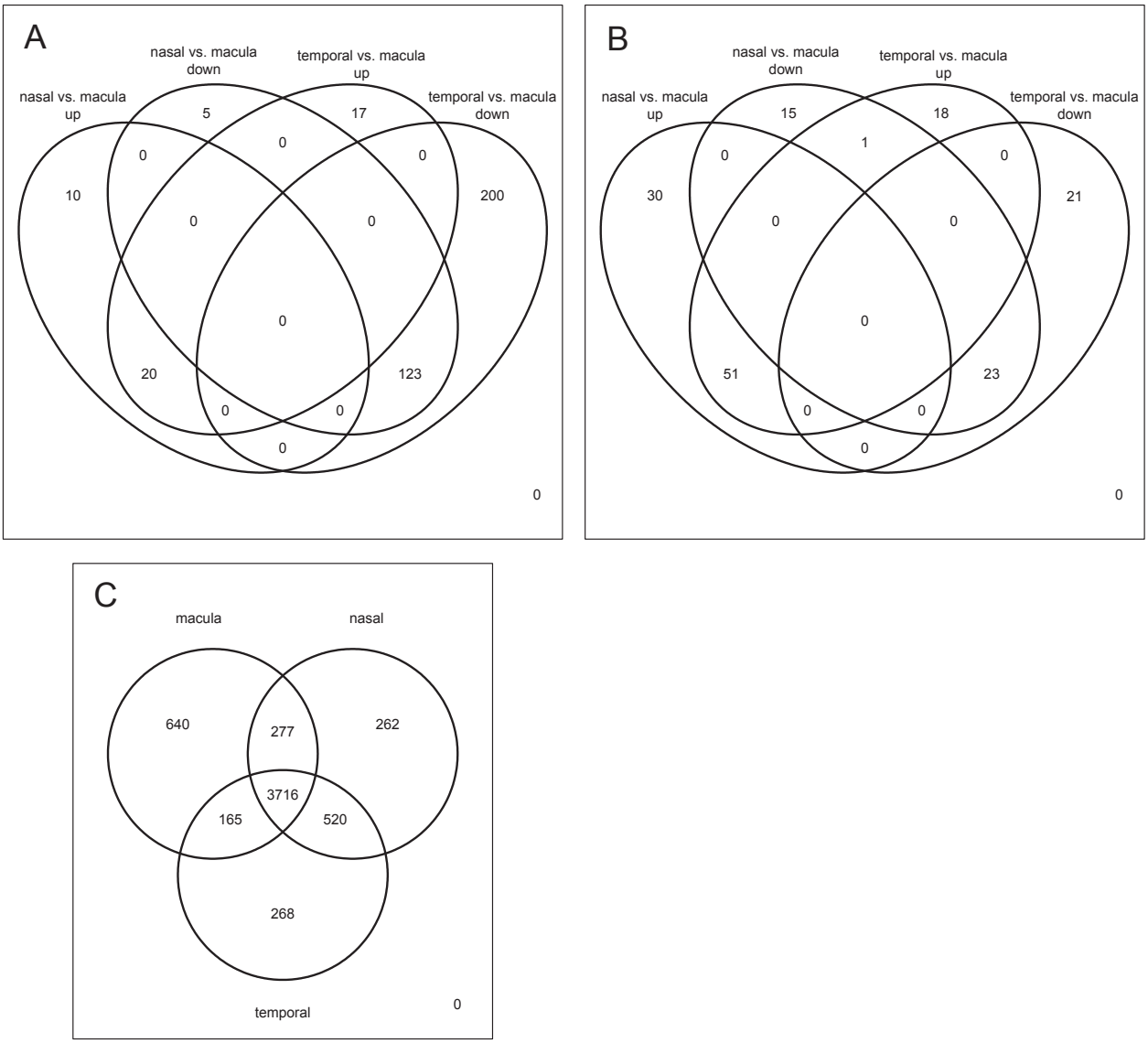

Fig. 3. Intersection between differentially expressed genes sets. (A) Regional pairwise comparisons in the retina. (B) Regional pairwise comparisons in the RPE/choroid. (C) RPE/choroid compared to retina for each region without respect to direction of fold change.

vs. temporal retina (Table 9). Fig. 3 shows the overlaps between differentially expressed genes in these comparisons.

3.3. Regional expression differences for specific retinal cell types

To explore regional differences in cell types in the retina, we mapped 92 genes identified by Siegert and coworkers as cell type specific in mouse retina (Siegert et al., 2012) to 78 human genes in our dataset (we required genes with human homologs to be expressed above FPKM 0 in at least half of our human retina samples). As indicated in Fig. 4, all four macula samples cluster together, while nasal and temporal samples are intermixed. All photoreceptor genes are enriched in the peripheral samples, whereas several genes of ganglion cell and amacrine cells are interleaved in a macula-enriched cluster.

3.4. RPE-specific and endothelium associated gene expression in the RPE/choroid

To compare cell populations in the RPE/choroid, we selected predefined RPE-specific and endothelium associated genes sets (Whitmore et al., 2013) and assessed trends in expression across temporal, macular, and nasal RPE/choroid punches (Fig. 5). The RPE-specific set shows an overall lower expression in the macula while the endothelium associated set shows higher expression in the macula.

3.5. Intradonor variation in five regions of the retina

In a separate experiment, we took retinal punches from macula, superior, inferior, temporal, and nasal regions of a single human donor eye and performed pairwise correlation for all genes expressed above FPKM 1 in a least one punch. Macula as compared to any of the peripheral punches showed the greatest dispersion

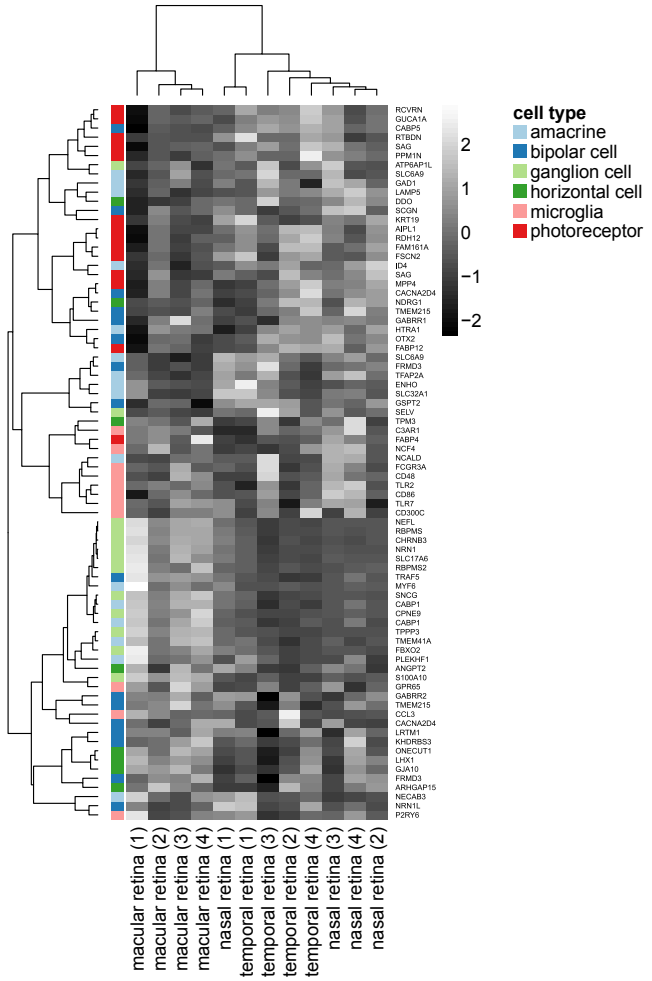

Fig. 4. Clustering of cell-type specific genes in the retina. Lighter shading indicates higher expression while darker shading indicates lower expression (FPKM values after row scaling). Hierarchical clustering was performed with complete linking on Spearman rank correlation distance.

from the diagonal (r from 0.97 to 0.98; Fig. 6). All peripheral vs. peripheral comparisons were also highly correlated, ($r = 0.99$), with modest dispersion from the diagonal in the superior vs. nasal and nasal vs. inferior comparisons.

4. Discussion

Here we present the first RNA-Seq dataset to separately investigate gene expression in the macula, nasal, and temporal human retina and RPE/choroid. While intriguing differences between the peripheral and the macular tissues were found, we did not observe significant differences between nasal and temporal retina. Only a few genes were differentially expressed between nasal and temporal RPE/choroid. Thus, the use of either nasal or temporal retina as general surrogates of "peripheral" retina seems warranted based on these data.

4.1. Limitations of the current study

RNA-Seq provides a wealth of data from each sample but interpreting these data remains challenging. The most commonly used measurement of expression, fragments per kilobase mapped per million reads (FPKM), should not be interpreted as a straightforward reflection of the number of RNA molecules within a given cell or tissue punch. Moreover, as any RNA-Seq derived expression estimate is fundamentally based on digital read counts, Gaussian models used for microarray analysis do not apply. To reduce false positives, we selected stringent thresholds for calling a gene as differentially expressed, likely missing some biologically relevant true positive events. Several neural retina genes, including *RHO*, *RCVRN*, and *SAG*, showed increased expression in the nasal RPE/choroid. This is likely due to incomplete separation of neural retina from the RPE during dissection, a problem widely reported in previous studies of ocular gene expression. Moreover, a larger sample size may provide enough power to detect transcriptome-level difference between nasal and temporal retina. However, despite our sample size, our data showed strong rank correlations with published FPKM values of peripheral and macular retina and RPE/choroid/sclera (Li et al., 2014).

4.2. Molecular determinants of the macula

Identifying the molecular determinants of the macular-peripheral distinction remains an open challenge in vision research. We found several transcription factors that were differentially expressed in the macula and periphery. For instance, *FOXI3* was upregulated in the nasal retina compared to the macular retina, whereas *IRX2* was downregulated in this comparison. *SIX2* was upregulated in the temporal retina compared to the macular retina, whereas *POU4F1*, *POU4F2*, *IRX1*, and *IRX2* were downregulated in this comparison. *POU4F1* and its target, *RIT2* (Zhang et al., 2013), are enriched in retinal ganglion cells (Kim et al., 2006), and both genes were significantly enriched in our macular retina samples. *RIT2* is also expressed in the mouse inner nuclear layer (Zhang et al., 2013).

4.3. Implications for vasculature in the retina and RPE/choroid

We observed decreased expression of prolactin (*PRL*) in the macular neuroretina as compared to either peripheral region. Prolactin is anti-angiogenic in the retina (Aranda et al., 2005), and systemic prolactin levels correlate with diabetic retinopathy (Arnold et al., 2010). Previous studies in rats and green monkeys have shown that PRL is expressed throughout the cell layers of the neural retina, and its receptor, PRLR, is expressed in photoreceptor nuclei, inner nuclear layer, and ganglion cell layer (Rivera et al., 2008). To our knowledge, this is the first dataset showing macular-peripheral differential expression of *PRL* in the retina. Distribution of *PRL* and other regulators of angiogenesis may help to explain the tendency of choroidal neovascular membranes to grow towards the fovea (Klein et al., 1989; de Jong, 2006), particularly if the neovascular membrane had breached the RPE or if RPE barrier function was compromised.

Of our predefined endothelium associated gene set, *MGP* (matrix Gla protein) showed the highest expression in the RPE/choroid. MGP may prevent calcification in the choroidal stroma or in Bruch's membrane (Booij et al., 2010). Recently, Gonzalez and coworkers used the *MGP* promoter to drive expression of β-galactosidase in a gene vector in anterior pole cultures of human donor eyes (Gonzalez et al., 2004). They observed localized expression in the trabecular meshwork (Gonzalez et al., 2004). However, they did not examine the tissues of the posterior pole. The Ocular Tissue Database (Wagner et al., 2013) entry for *MGP* (available at https://genome.uiowa.edu/otdb/) shows relatively high expression in the RPE/choroid, on par with the trabecular meshwork, ciliary body, and iris, and low expression in the retina, consistent with our findings. Further study will be needed to determine the extent to which MGP contributes to Bruch's membrane and/or choroidal elasticity.

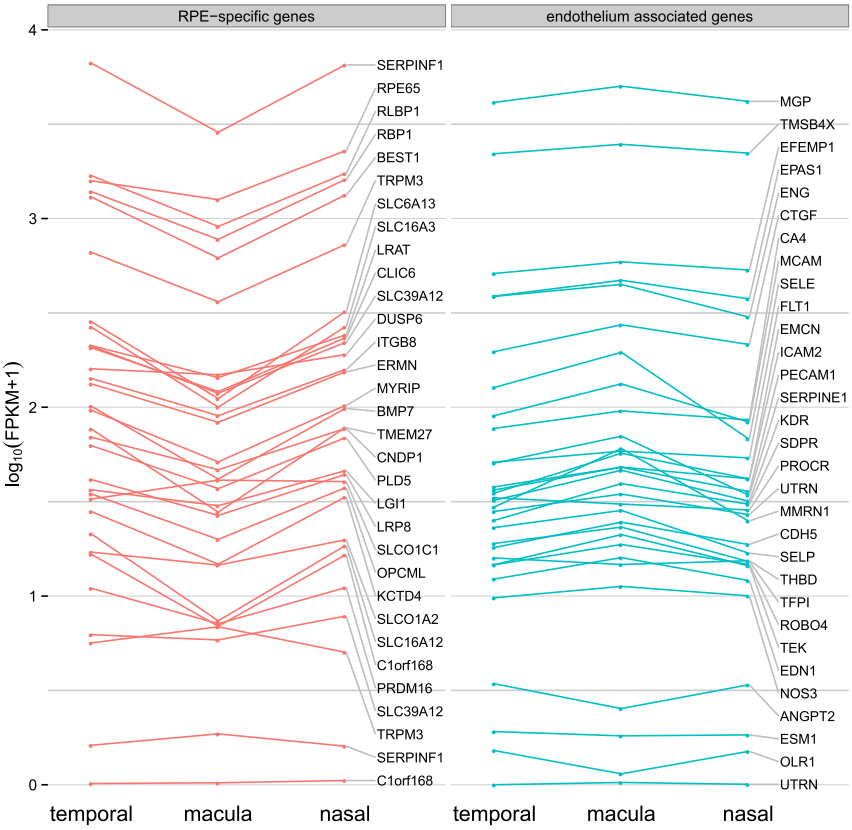

Fig. 5. Expression of RPE-specific and endothelium associated gene sets across regions of the RPE/choroid.

4.4. Comparison with previously published data

We also observed robust expression of *TIMP3* in our dataset, compared to FPKM values of 0 in the RPE/choroid in that of Li et al. These authors noted that expression of *TIMP3* was almost entirely limited to the retina. This result may be a side effect of the algorithm used by Cufflinks. When Cufflinks estimates FPKM values, it first computes "fragment bundles." Extremely high bundle values can cause difficulty for the algorithm; thus, Cufflinks labels such genes as "HIDATA" and does not estimate FPKMs. In our initial analysis, we failed to detect *RHO* in both nasal and temporal retina. However, inspection of individual alignment files for these samples showed robust expression, with read counts in excess of 40,000 across the *RHO* transcript in temporal samples (Supplemental Figure S1). Further investigation revealed that identified expression of *TTR* also marked by the "HIDATA" criterion in the nasal RPE/choroid. Setting the "–max_bundle_frags" parameter for Cufflinks and Cuffdiff to an arbitrarily high value (e.g., 20,000,000) removed the "HIDATA" label, resulting in FPKM estimates for *RHO* and *TTR* in all groups.

4.5. Utility of ophthalmic expression datasets

Linkage studies have identified many disease loci in families affected by macular dystrophies or other eye diseases (see examples at RetNet [https://sph.uth.edu/retnet/] and Online Mendelian Inheritance in Man [http://omim.org/]). Causative mutations have yet to be pinpointed within several of these loci, which cover megabases of the genome and contain dozens of genes. Multi-tissue regional ophthalmic datasets, such as we present here, may help reduce the search space for candidate genes, especially for diseases with region-specific or tissue-specific phenotypes. Moreover, as more Mendelian diseases with coding mutations are solved, identifying silent mutations and changes in regulatory regions is the remaining frontier for molecular genetics. For instance, in 2002 Schulz and coworkers examined *NPVF* (formerly *C7orf9*) for coding sequence changes that could explain Cystoid Macular Edema (chr7:7,300,000–28,800,000; OMIM 153880). They found no deleterious SNPs in the coding sequence of NPVF, but they acknowledged that the promoter sequence may harbor the causative mutation (Schulz et al., 2002). In our data, we observe significant macular enrichment of *NPVF* as compared to both nasal and temporal retina, suggesting that promoter changes could alter the region-specific expression of *NPVF* in the retina.

MAK-related RP (OMIM 614181) tends to spare the temporal retina while damaging the inferior and nasal retina (Stone et al., 2011; Tucker et al., 2011). While we observed lower expression of MAK in the macula (Fig. 7A), similar to many other photoreceptor cell specific genes (Fig. 4), differences in peripheral regions of the retina were not detected. This suggests that the regional degeneration observed in *MAK*-related RP is likely due to the distribution of substrates or factors regulating *MAK* function rather than differences in gene expression across retinal topography.

BEST1, the gene mutated in Best vitelliform macular dystrophy (OMIM 153700), has previously been shown to be expressed at lower levels in the macular RPE/choroid than in the periphery by immunohistochemistry, quantitative PCR, and proteomics (Mullins et al., 2007; Skeie and Mahajan, 2014). We observed a similar pattern of expression in our data (Figs. 5 and 7B). However, comparable profiles were seen for many other RPE-specific genes, including *RPE65*, a gene previously shown to have relatively equal abundance between macular and peripheral RPE/choroid (Kociok

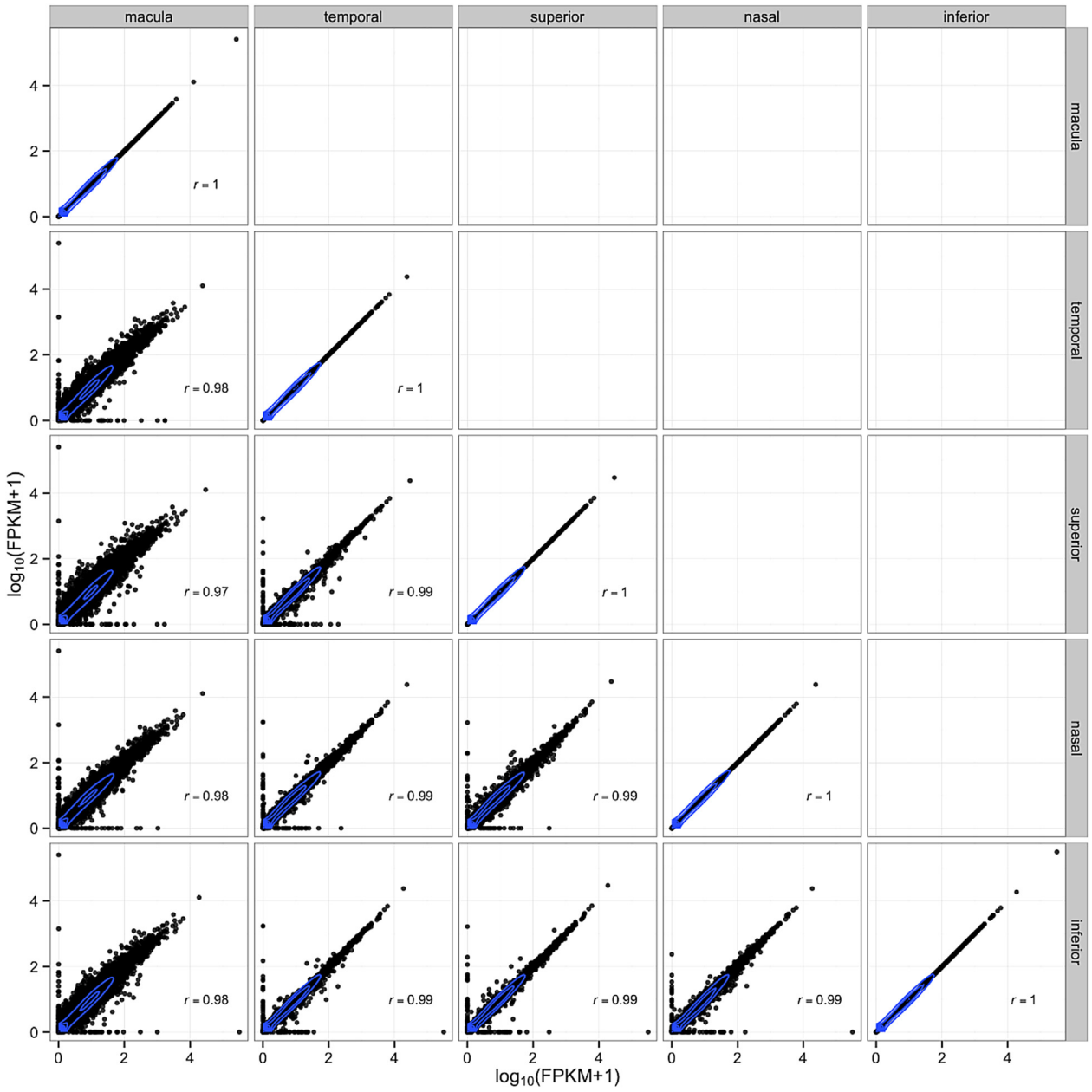

Fig. 6. Intradonor region variability across five regions of the retina.

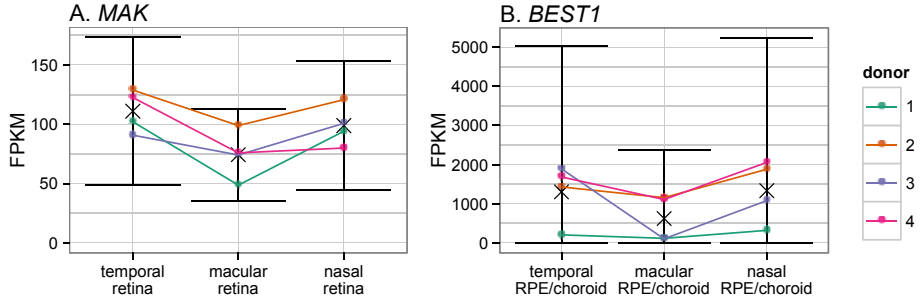

Fig. 7. Expression of *MAK* (retina) and *BEST1* (RPE/choroid) across regions. Mean indicated by (×). Error bars denote 95% confidence intervals for abundance as calculated by Cuffdiff.

and Joussen, 2007). One implication of these findings, as depicted in Fig. 5, is that normalization should be performed using cell-type specific genes with relatively consistent expression across anatomic regions.

5. Conclusion

We have presented a comprehensive, transcriptome-wide view of gene expression across the neural retina and RPE/choroid in three regions of the retina. Gene expression in the retina correlates with the anatomic distribution of rod photoreceptors and ganglion cells in the macula and periphery. RPE-specific and endothelium associated gene expression in the RPE/choroid appear inversely related, with RPE-specific genes expressed at a lower level in the macula than at the periphery, whereas endothelium associated genes show slightly higher expression in the macula than in the periphery. Additional RNA-Seq datasets for ophthalmic tissues will facilitate more complex analyses, including mapping retina-specific transcriptional regulatory circuits and identifying lowly expressed exons.

Both analyses will facilitate the search for novel disease causing mutations. For example, we previously used the five region RNA-Seq data to identify rare alternative exons in *ABCA4*, screened a cohort of patients with clinical evidence of *ABCA4* disease for variants in these exons, and identified novel splice-site mutations not found in controls (Braun et al., 2013). To advance similar studies, we are making our samples available on the database of Genotypes and Phenotypes (dbGAP).

Acknowledgments

This project was supported by NIH Health Grants EY023187 (TES), EY024605 (RFM), EY016822 (EMS), and DP2-OD007483-01 (BAT), the Howard Hughes Medical Institute (EMS), The Elmer and Sylvia Sramek Charitable Foundation (RFM/BAT), the Hansjoerg EJW Kolder MD, PhD Professorship for Best Disease (RFM), and Vision for Tomorrow. This research was supported in part through computational resources provided by The University of Iowa, Iowa City, Iowa.

Appendix A. Supplementary data

Supplementary data related to this article can be found at http://dx.doi.org/10.1016/j.exer.2014.11.001.

References

Aranda, J., Rivera, J.C., Jeziorski, M.C., Riesgo-Escovar, J., Nava, G., López-Barrera, F., et al., 2005 Aug. Prolactins are natural inhibitors of angiogenesis in the retina. Investigative Ophthalmol. Vis. Sci. 46 (8), 2947–2953.

Arnold, E., Rivera, J.C., Thebault, S., Moreno-Páramo, D., Quiróz-Mercado, H., Quintanar-Stéphano, A., et al., 2010 Dec. High levels of serum prolactin protect against diabetic retinopathy by increasing ocular vasoinhibins. Diabetes 59 (12), 3192–3197. PMCID: PMC2992782.

Booij, J.C., Baas, D.C., Beisekeeva, J., Gorgels, T.G.M.F., Bergen, A.A.B., 2010 Jan. The dynamic nature of Bruch's membrane. Prog. Retin. Eye Res. 29 (1), 1–18.

Bowes Rickman, C., Ebright, J.N., Zavodni, Z.J., Yu, L., Wang, T., Daiger, S.P., et al., 2006 Jun. Defining the human macula transcriptome and candidate retinal disease genes using EyeSAGE. Investigative Ophthalmol. Vis. Sci. 47 (6), 2305–2316. PMCID: PMC2813776.

Braun, T.A., Mullins, R.F., Wagner, A.H., Andorf, J.L., Johnston, R.M., Bakall, B.B., et al., 2013. Non-exomic and synonymous variants in ABCA4 are an important cause of Stargardt disease. Hum. Mol. Genet. 22 (25), 5136–5145.

Curcio, C.A., Allen, K.A., 1990 Oct 1. Topography of ganglion cells in human retina. J. Comp. Neurology 300 (1), 5–25.

Curcio, C.A., Sloan, K.R., Kalina, R.E., Hendrickson, A.E., 1990 Feb 22. Human photoreceptor topography. J. Comp. Neurology 292 (4), 497–523.

de Jong, P.T.V.M., 2006 Oct 5. Age-related macular degeneration. N. Engl. J. Med. 355 (14), 1474–1485.

DeLuca, D.S., Levin, J.Z., Sivachenko, A., Fennell, T., Nazaire, M.-D., Williams, C., et al., 2012 Jun 1. RNA-SeQC: RNA-seq metrics for quality control and process optimization. Bioinformatics 28 (11), 1530–1532. PMCID: PMC3356847.

Diehn, J.J., Diehn, M., Marmor, M.F., Brown, P.O., 2005. Differential gene expression in anatomical compartments of the human eye. Genome Biol. 6 (9), R74. PMCID: PMC1242209.

Gonzalez, P., Caballero, M., Liton, P.B., Stamer, W.D., Epstein, D.L., 2004 May. Expression analysis of the matrix GLA protein and VE-cadherin gene promoters in the outflow pathway. Investigative Ophthalmol. Vis. Sci. 45 (5), 1389–1395.

Ishibashi, K., Tian, J., Handa, J.T., 2004 Sep. Similarity of mRNA phenotypes of morphologically normal macular and peripheral retinal pigment epithelial cells in older human eyes. Investigative Ophthalmol. Vis. Sci. 45 (9), 3291–3301.

Jonas, J.B., Schneider, U., Naumann, G.O., 1992. Count and density of human retinal photoreceptors. Graefes Arch. Clin. Exp. Ophthalmol. 230 (6), 505–510.

Kim, C.Y., Kuehn, M.H., Clark, A.F., Kwon, Y.H., 2006. Gene expression profile of the adult human retinal ganglion cell layer. Mol. Vis. 12, 1640–1648.

Kim, D., Pertea, G., Trapnell, C., Pimentel, H., Kelley, R., Salzberg, S.L., 2013 Apr 25. TopHat2: accurate alignment of transcriptomes in the presence of insertions, deletions and gene fusions. Genome Biol. 14 (4), R36.

Klein, M.L., Jorizzo, P.A., Watzke, R.C., 1989 Sep. Growth features of choroidal neovascular membranes in age-related macular degeneration. Ophthalmology 96 (9), 1416–1419 discussion1420–1.

Kociok, N., Joussen, A.M., 2007 Jan. Varied expression of functionally important genes of RPE and choroid in the macula and in the periphery of normal human eyes. Graefes Arch. Clin. Exp. Ophthalmol. 245 (1), 101–113.

Li, M., Jia, C., Kazmierkiewicz, K.L., Bowman, A.S., Tian, L., Liu, Y., et al., 2014. Comprehensive analysis of gene expression in human retina and supporting tissues. Hum. Mol. Genet. 23 (15), 4001–4014.

Mullins, R.F., Kuehn, M.H., Faidley, E.A., Syed, N.A., Stone, E.M., 2007 Jul. Differential macular and peripheral expression of bestrophin in human eyes and its implication for Best disease. Investigative Ophthalmol. Vis. Sci. 48 (7), 3372–3380.

Radeke, M.J., Peterson, K.E., Johnson, L.V., Anderson, D.H., 2007 Sep. Disease susceptibility of the human macula: differential gene transcription in the retinal pigmented epithelium/choroid. Exp. Eye Res. 85 (3), 366–380.

Rivera, J.C., Aranda, J., Riesgo, J., Nava, G., Thebault, S., López-Barrera, F., et al., 2008 Feb. Expression and cellular localization of prolactin and the prolactin receptor in mammalian retina. Exp. Eye Res. 86 (2), 314–321.

Rouhani, F., Kumasaka, N., de Brito, M.C., Bradley, A., Vallier, L., Gaffney, D., 2014 Jun. Genetic background drives transcriptional variation in human induced pluripotent stem cells. PLoS Genet. 10 (6), e1004432. PMCID: PMC4046971.

Schulz, H.L., Stoehr, H., White, K., van Driel, M.A., Hoyng, C.B., Cremers, F., et al., 2002 Mar 19. Genomic structure and assessment of the retinally expressed RFamide-related peptide gene in dominant cystoid macular dystrophy. Mol. Vis. 8, 67–71.

Siegert, S., Cabuy, E., Scherf, B.G., Kohler, H., Panda, S., Le, Y.-Z., et al., 2012 Mar. Transcriptional code and disease map for adult retinal cell types. Nat. Neurosci. 15 (3), 487–495. S1–2.

Skeie, J.M., Mahajan, V.B., 2014 Jul 24. Proteomic landscape of the human choroid-retinal pigment epithelial complex. JAMA Ophthalmol. (in press).

Stone, E.M., Luo, X., Héon, E., Lam, B.L., Weleber, R.G., Halder, J.A., et al., 2011 Dec. Autosomal recessive retinitis pigmentosa caused by mutations in the MAK gene. Investigative Ophthalmol. Vis. Sci. 52 (13), 9665–9673. PMCID: PMC3341124.

Trapnell, C., Hendrickson, D.G., Sauvageau, M., Goff, L., Rinn, J.L., Pachter, L., 2013. Differential analysis of gene regulation at transcript resolution with RNA-seq. Nat. Biotechnol. 31 (1), 46–53.

Trapnell, C., Roberts, A., Goff, L., Pertea, G., Kim, D., Kelley, D.R., et al., 2012. Differential gene and transcript expression analysis of RNA-seq experiments with TopHat and Cufflinks. Nat. Protoc. 7 (3), 562–578. PMCID: PMC3334321.

Trapnell, C., Williams, B.A., Pertea, G., Mortazavi, A., Kwan, G., van Baren, M.J., et al., 2010 May. Transcript assembly and quantification by RNA-Seq reveals unannotated transcripts and isoform switching during cell differentiation. Nat. Biotechnol. 28 (5), 511–515. PMCID: PMC3146043.

Tucker, B.A., Scheetz, T.E., Mullins, R.F., DeLuca, A.P., Hoffmann, J.M., Johnston, R.M., et al., 2011 Aug 23. Exome sequencing and analysis of induced pluripotent stem cells identify the cilia-related gene male germ cell-associated kinase (MAK) as a cause of retinitis pigmentosa. Proc. Natl. Acad. Sci. 108 (34), E569–E576. PMCID: PMC3161526.

van Soest, S.S., de Wit, G.M.J., Essing, A.H.W., Brink ten, J.B., Kamphuis, W., de Jong, P.T.V.M., et al., 2007. Comparison of human retinal pigment epithelium gene expression in macula and periphery highlights potential topographic differences in Bruch's membrane. Mol. Vis. 13, 1608–1617.

Wagner, A.H., Anand, V.N., Wang, W.-H., Chatterton, J.E., Sun, D., Shepard, A.R., et al., 2013 Jun. Exon-level expression profiling of ocular tissues. Exp. Eye Res. 111, 105–111. PMCID: PMC3664108.

Whitmore, S.S., Braun, T.A., Skeie, J.M., Haas, C.M., Sohn, E.H., Stone, E.M., et al., 2013. Altered gene expression in dry age-related macular degeneration suggests early loss of choroidal endothelial cells. Mol. Vis. 19, 2274–2297. PMCID: PMC3834599.

Zhang, L., Wahlin, K., Li, Y., Masuda, T., Yang, Z., Zack, D.J., et al., 2013. RIT2, a neuron-specific small guanosine triphosphatase, is expressed in retinal neuronal cells and its promoter is modulated by the POU4 transcription factors. Mol. Vis. 19, 1371–1386. PMCID: PMC3692409.